



Kinetics and isotherms of dichlorodiphenyltrichloroethane (DDT) adsorption using soil–zeolite mixture

Sarah Mustafa Ahmed¹ · Mohd Raihan Taha² · Omer Muhie Eldeen Taha³ 

Received: 13 September 2017 / Accepted: 10 December 2017 / Published online: 20 December 2017
© Springer International Publishing AG, part of Springer Nature 2017

Abstract

Soil contaminated by organic pollutants such as dichlorodiphenyltrichloroethane (DDT) is an environmental concern due to the strong sorption of organochlorine pesticide onto the soil matrix and persistence in the environment. The remediation of contaminated soils with organochlorine pesticide using nanotechnology is an innovative technology for speeding up this process. This work presents a study of adsorption of DDT onto the zeolite surface. Experiments were conducted using batch adsorption procedures at different DDT concentrations, from 5 to 50 mg/L, and the amount of the zeolite used was 0.1, 0.5, 0.8, and 1.2 g. Results show that the zeolite has a moderate adsorption capacity for the DDT, and the highest adsorption capacity obtained from this study was about 30%. However, the percentage of adsorption can be increased significantly with the increase in the amount of the zeolite in samples. Also, adsorption kinetics and adsorption isotherms were applied. Five different kinetic models, i.e., pseudo-first-order kinetic model, the pseudo-second-order kinetic model, intraparticle diffusion model, Elovich kinetic model, and Bangham kinetic model were used to fit the kinetic data. The result shows that the pseudo-second-order model represented the best fits to the experiments. The adsorption isotherms were determined using three different models as well, i.e., Freundlich, Langmuir, and Temkin. The best-fitted adsorption isotherm models were found to be in both Langmuir and Freundlich. Moreover, results show that the effectiveness of treatment process is highly affected by pH. Increasing the pH has a negative effect on the adsorption process, and best uptake of DDT was noted in acidic media at pH 3.

Keywords Adsorption kinetics · Adsorption isotherm · DDT · Soil contamination

Introduction

Soil contamination is the accumulation in soils of persistent toxic compounds, chemicals, solid or liquid hazardous substances, radioactive materials, salts, or disease-causing agents, which have adverse effects on human health, plant

growth, and animal health. However, soil can be polluted by seepage from a landfill, discharge of industrial waste into the soil, and percolation of contaminated water into the soil [1–3]. Soil pollution includes the pollution of soils with materials, mostly due to chemicals that are present at concentrations higher than normal which may cause harm to the environment. The most common chemicals involved in causing soil pollution are petroleum hydrocarbons, heavy metals, pesticides, and solvents [4]. Soil pollution also can cause severe impact on agriculture and thus affect the quality and quantity of agricultural yields [5, 6]. Contamination of soil from the use of pesticides is one of the most pollution source threats to the environment. The use of pesticides in agriculture is still one of the most important problems of soil pollution [7]. Also, it affects the fertility of the soil and eventually leads to the contamination, to harm humans and animals through eating contaminated plants [8]. The chlorinated pesticides such as dichlorodiphenyltrichloroethane (DDT) do not degrade quickly and remain for an extended period

✉ Sarah Mustafa Ahmed
sarah.mustafa@tu.edu.iq

Mohd Raihan Taha
drmr@eng.ukm.my

Omer Muhie Eldeen Taha
omarmahie@yahoo.com

¹ Department of Civil Engineering, University of Tikrit, Tikrit, Iraq

² Department of Civil and Structural Engineering, Universiti Kebangsaan Malaysia, 43600 UKM Bangi, Selangor, Malaysia

³ Department of Civil Engineering, University of Kirkuk, Kirkuk, Iraq

[9]. Soil contaminated with persistent organic pollutants (POPs), especially chlorinated aromatic compounds such as DDT, is an environmental issue because of the high sorption of organochlorine pesticides onto the soil matrix and persistence in the environment [10].

The most problems of soil contamination by DDT are an entry into the food chain where they can affect human and animal adversely and exposure by workers to chlorinated organic pesticides (OCPs) when pesticides sprayed [11]. Soils are also considered the main sinks of persistent organic pollutants (POPs) and play a fundamental role in the global cycling [12, 13].

Dichlorodiphenyltrichloroethane (DDT) or [1,1,1-trichloro-2,2-bis(4-chlorophenyl) ethane] is a chlorohydrocarbon, which is an organochlorine pesticide (OCP), is a typical persistent organic pollutant (POP). Because of its persistence, low volatility, bioaccumulation potential, and high toxicity, it is a major environmental issue, receiving considerable attention by scientists and the public [14]. DDT is insoluble in water and soluble in most organic solvents. It is semi-volatile and can be expected to split into the atmosphere consequently. It is existed everywhere in the environment, and residues found in inaccessible regions such as the Arctic [15]. DDT has been widely used as an insecticide to control mosquito-borne malaria and typhus [16]. DDT offered after Second World War as the simplest and the best solution to pest problems [17]. It was among the first chemicals used widely as an insecticide to control diseases that spread by mosquito such as malaria and typhus [16]. According to Sharma [1], dichlorodiphenyltrichloroethane (DDT) beside polychlorinated biphenyls (PCBs) is the most dangerous pollutants in soil, which comes from industrial wastes [1]. The presence of chlorine atoms in DDT and its metabolites makes them highly toxic to higher organisms [18]. As a result of its lipophilic properties, DDT has a high bioaccumulation potential, especially in birds of prey. It magnifies in animals through the food chain. It is also quite resistant the metabolic processes to a large degree [19]. DDT and its metabolites can be adsorbed on the surface of the soil or particulates in the water and become sediment in the end. DDT is very persistent in the environment, and thus, as much as 50% DDT can stay in the soil after 10–15 years of use [20, 21]. This persistence, along with high solubility in lipids, provides the necessary conditions for DDT to concentrate in organisms. DDT and its metabolites have been detected in all compartments (air, water, soil, and living organisms) in remote areas [15]. However, the half-life of DDT is estimated to be around 15 years in soil [22] and can be changed depending on the soil conditions [23]. It is found that the DDT concentration in the contaminated soil exceeds the limit set by national soil quality standards in some regions (i.e., in Tianjin area, the concentration of DDT was 7.5 ng/g) [24].

Over the years, the field of remediation has grown and evolved, continually developing and adopting modern technologies in an attempt to improve the remediation process.

Nano-materials are introduced in different studies area such as electric, chemical and environmental [25, 26]. Due to the reacting ability of nanoparticles coming from the high surface area of the nanoparticles, nano-materials can produce extremely high improvement performance. In a recent study by Varanasi et al. [27], the results showed that nanoparticles help in the process of removal of chlorine and high PCB destruction efficiencies. The destruction efficiency can be increased during the preliminary treatment (mixing of soil and iron nanoparticles in water) by increasing the temperature of the water. Ultimate thermal destruction of soil-bound PCBs takes place at 300 °C in air. A minimum destruction of PCBs accomplished by this method is 95%. The zeolites have been extensively studied over the last 10 years because of attractive properties such as molecular sieving, the high cation exchange capacity, and affinity for heavy metals [28]. Natural zeolites were used in the field of the protection of the environment against radioactive contamination as buffer materials for the pollution [29]. Insulating properties of natural zeolites led to use it as lining for landfills. With the use of natural zeolites as a substitute for the clay liner would reduce the thickness of the lining and reduce the risk of leachate into the groundwater. Zeolite, an inorganic ion exchanger, may be used as a suitable technical–economical solution for water treatment [30]. According to Tahir, Uddin [31], the zeolite-3A could be utilized as a potential source for the removal of lead from metal electroplating industries waste before discharging into hydrosphere. The results obtained show that the lead can be removed quantitatively (99.9%) by using zeolite-3A. In the field of treatment and control of heavy metal in the environment, zeolite has been used extensively for the remediation of hazardous heavy metal polluted soils [32]. Zeolite is considered as important remediation agent for restriction and prevents mobilization of heavy metals in soils, which can decrease the bioavailability of heavy metals in soils [33]. Moreover, zeolite has been used to clean up Zn, V, Cd, and Hg ions from textile fabric waste waters [34]. Also, zeolites can remove both hydrophilic and hydrophobic organics depending on their Si/Al ratio [35, 36].

This research deals with the use of zeolite to clean up a Malaysian residual soil. The main objective of this study is to evaluate the performance of zeolite for removal of DDT from contaminated soil.

Adsorption mechanism

Adsorption kinetics

Adsorption is one of the most widely applied technologies for removing pollutants from contaminated environments. Its kinetics is of great importance to assess the performance of a specific adsorbent and to understand the underlying

mechanisms [37]. The kinetics of adsorption describes the adsorbate rate of uptake on the adsorbent and it controls the equilibrium time [38]. Also, the kinetics describes the solute uptake rate which in turn controls the residence time of sorbet uptake at the solid–solution interface [39]. The kinetic parameters are helpful for the prediction of adsorption rate, which gives valuable information for designing and modeling the processes. Previously, several mathematical models have been proposed to describe adsorption data. They are applied to describe the kinetic process of adsorption [37, 40]. Most of the sorption/desorption transformation processes of various solid phases are time dependent. To understand the dynamic interactions of pollutants with solid phases and to predict their fate with time, knowledge of the kinetics of these processes is important [41]. To identify the key process controlling the adsorption rate, several models must check for suitability and consistency over a broad range of the system parameters. In this study, the kinetics of the adsorption data was analyzed using five different kinetic models: pseudo-first- and pseudo-second-order models, intraparticle diffusion model, and Elovich kinetic model and Bangham equations, which are all extensively used in kinetic studies.

Pseudo-first-order model

The pseudo-first-order kinetic model is a simple kinetic analysis of adsorption which has been widely used to predict adsorption kinetics. The adsorption kinetics using pseudo-first-order model is given in Eq. 1 [37, 42–44].

$$\ln\left(\frac{q_e}{q_e - q_t}\right) = k_1 t \quad (1)$$

It can be rewritten as:

$$\ln(q_e - q_t) = \ln q_e - k_1 t \quad (2)$$

where q_e and q_t (mg/kg) are the amounts of adsorbate adsorbed at equilibrium time and at any time t (h), respectively. The constant k_1 (1/h) is the adsorption rate constant of pseudo-first-order reaction.

Pseudo-second-order kinetic model

A pseudo-second-order equation was derived based on equilibrium adsorption capacity [45]. The adsorption kinetics described by the pseudo-second-order kinetic model is given in Eq. 3 [37, 39, 44, 46].

$$\frac{1}{(q_e - q_t)} = \frac{1}{q_e} + k_2 t \quad (3)$$

which can rearrange as follows:

$$\frac{t}{q_t} = \frac{1}{k_2 q_e^2} + \frac{t}{q_e} \quad (4)$$

where q_e and q_t (mg/kg) were previously defined and the constant k_2 (kg/mg h) is the adsorption rate constant of pseudo-second-order adsorption.

Intraparticle diffusion model

The intraparticle diffusion model refers to the theory proposed by Weber and Morris [47]. According to Weber and Morris [47], many adsorption cases vary almost proportionally with $t^{\frac{1}{2}}$ rather than with the contact time t . The intraparticle diffusion model proposed by Weber and Morris [47] provided the rate for intraparticle diffusion by a relationship between q_t and square root of time, $t^{\frac{1}{2}}$, as shown in Eq. 5 [37, 44, 45, 48].

$$q_t = k_3 t + C_i \quad (5)$$

where k_3 (mg/kg h^{0.5}) is the intraparticle diffusion rate constant and C_i is associated with the boundary layer thickness. If intraparticle diffusion occurs, then q_t versus $t^{\frac{1}{2}}$ will be linear, and if the plot passes through the origin, then the rate limiting process is only due to the intraparticle diffusion. Otherwise, some other mechanism along with intraparticle diffusion is also involved. Previous studies showed that the curves following intraparticle diffusion have three various stages, i.e., initial very fast surface adsorption (external mass transfer) followed by gradual adsorption stage where the intraparticle diffusion is rate-controlled. Finally, a plateau shows equilibrium sorption where intraparticle diffusion is very slow due to low solute concentrations in the solution [39, 45].

Elovich kinetic model

Elovich kinetic model was proposed by Zeldowitsch [49]. This model assumes heterogeneous active sites of adsorbent and different activation energies for sorption of organics such as dye molecules. It is given by Eq. 6 as follows [37]:

$$\frac{dq_t}{dt} = \alpha e^{-\beta q_t} \quad (6)$$

Integrating Eq. 6 with boundary condition of $q_t = 0$ at $t = 0$ and $q_t = t$ at $t = t$, the above equation becomes:

$$q_t = \frac{1}{\beta} \ln(\alpha \cdot \beta) + \frac{1}{\beta} \ln t \quad (7)$$

where α is the initial rate of adsorption (mg kg⁻¹ min⁻¹) and β is desorption rate constant for this adsorption. The values of α and β are obtained from the slope and intercept of linear trend lines of q_t against $\ln t$.

Bangham kinetic model

This kinetic equation is given by

$$q_t = k_t t^{\frac{1}{m}} \quad (8)$$

The linear form of this model is given by

$$\ln(q_t) = \ln(k_t) + \frac{1}{m} \ln(t) \quad (9)$$

where k_t is rate constant for sorption and $\frac{1}{m}$ measures the intensity of sorption. The nonlinear fitting of q_t against t using Eq. 8 or linear plot of $\ln(q_t)$ against $\ln(t)$ gives the values of rate constant k_t and m . If the experimental data are represented by this equation, then the adsorption kinetics are limited by the pore diffusion [50].

Adsorption isotherms

Adsorption isotherms are mathematical models that describe the distribution of the adsorbate species among liquid and solid phases, based on a set of assumptions that are related to the heterogeneity/homogeneity of the solid surface, the type of coverage, and the possibility of interaction between the adsorbate species [41]. The equilibrium isotherms are important for understanding the adsorption systems. Adsorption isotherm reflects the relationship between the amount of a solute adsorbed at constant temperature and its concentration in the equilibrium solution. It provides essential physicochemical data for assessing the applicability of the adsorption process as a complete unit operation [51].

There are several isotherm equations available for analyzing experimental adsorption equilibrium data. In this work, three adsorption isotherms, Langmuir, Freundlich, and Temkin, were applied to fit the equilibrium data of adsorption of DDT onto zeolite.

Langmuir isotherm

Langmuir model assumes that the absorption occurs on the surface of a homogeneous by monolayer adsorption without any interaction between adsorbed ions [41]. The nonlinear and linear form of this isotherm is given by Eqs. 10 and 11, respectively.

$$q_e = \frac{q_{\max} k_1 C_e}{1 + k_1 C_e} \quad (10)$$

$$\frac{1}{q_e} = \frac{1}{q_{\max} k_1 C_e} + \frac{1}{q_{\max}} \quad (11)$$

where k_1 is the Langmuir constant and q_{\max} is maximum adsorption capacity.

Freundlich isotherm

The Freundlich equation is an empirical equation based on adsorption on a heterogeneous surface [41]. The nonlinear and linear form of this equation is given by:

$$q_e = k_f C_e^{1/n} \quad (12)$$

$$\ln(q_e) = \ln(k_f) + \frac{1}{n} \ln(C_e) \quad (13)$$

where C_e (mg/L) is the equilibrium concentration and q_e (mg/g) is the amount adsorbed per unit mass of the adsorbent. k_f (L/g) is the Freundlich constant indicative of the relative adsorption capacity of the adsorbent. The constant n is the Freundlich equation exponent that represents the parameter characterizing quasi-Gaussian energetic heterogeneity of the adsorption surface. For linear adsorption, n is unity. When the adsorption is dominated by chemical sorption, the value of n becomes less than unity. A value of $n > 1$ indicates physical sorption [52].

Temkin isotherm

In this model, it is assumed that heat of sorption of the molecules on the adsorbent surface reduces linearly due to adsorbate–adsorbate interaction. The Temkin isotherm equation assumes that the heat of adsorption of all the molecules in layer decreases linearly with coverage due to adsorbent–adsorbate interactions and that the adsorption is characterized by a uniform distribution of the bonding energies, up to some maximum binding energy [53]. The nonlinear form of this model is given by

$$q_e = a + 2.303b \log(C_e) \quad (14)$$

where a (L/mg) is equilibrium binding constant corresponding to the maximum binding energy and b is related to the heat of adsorption. The isotherm constants a and b are determined from slope and intercept of straight-line plot of q_e against $\log(C_e)$.

Materials and methods

Materials

Soil

The soil selected for this study is residual soil in the campus University Kebangsaan Malaysia, Bangi, Selangor, Malaysia. The soil was cut from 0.3 to 0.6 m below the ground surface. In the laboratory, the soil was air-dried

for 20 days, then crashed using rubber pestle and sieved to remove roots and large particles to a particle size ≤ 2 mm, and then stored in polyethylene bags at room temperature.

Zeolite

The zeolite used in this study is a ferrierite zeolite with large particle basically. However, it has nano-pores in its physical structure. Thus, it can be classified as nanoparticles. In general, the average particle size of zeolite particles is 500 nm, and the specific surface area is $12 \text{ m}^2/\text{g}$. The basic zeolite properties are described in Table 1. The SEM image and the XRF result of the zeolite particle are shown in Fig. 1.

Dichlorodiphenyltrichloroethane (DDT)

DDT used in this research was 4,4'-DDT supplied by Sigma-Aldrich: Supelco (USA). Its formula is $(\text{ClC}_6\text{H}_4)_2\text{CHCCl}_3$. Other synonyms for 4,4'-DDT are

Table 1 Some typical properties of zeolite used in this study

Property	Data
Average particle size (nm)	500
Surface area (m^2/g)	12
Specific gravity	2.25
Cation change capacity (meq/100 g)	1.7
pH	7.88
<i>Chemical contents (%)</i>	
SiO_2	66
Al_2O_3	12.3
Fe_2O_3	5.9
CaO	3.17
Na_2O	1.8
MgO	1.72
K_2O	2.02

1,1,1-trichloro-2,2-bis(4-chlorophenyl)ethane and 1,1-bis(4-chlorophenyl)-2,2,2-trichloroethane. Some chemical properties of 4,4'-DDT are given in Table 2.

Solutions or reagents

***n*-Hexane** *n*-Hexane used in this study was also purchased from Sigma-Aldrich. Its molecular formula is $\text{CH}_3(\text{CH}_2)_4\text{CH}_3$. Some chemical properties of *n*-hexane are shown in Table 3.

Test procedure

Characterization tests of soil (chemical composition of soil, soil pH, specific gravity, liquid and plastic limits, sieve analysis, organic carbon content, cation exchange capacity, and surface area) were conducted. Sieve and hydrometer tests were carried out following ASTM D421 and ASTM D422, respectively. The pH of soil has been investigated according to British standard BS 1377: 1990. Moisture content test achieved in this study followed ASTM D2216. The liquid limit (LL) and plastic limit (PL) tests were carried out according to British standard BS 1377: 1990 using cone penetrometer. The specific gravity of soil solids was tested according to ASTM D854 by water pycnometer. The soil is classified as clayey sand (SC) according to unified

Table 2 Some typical properties of 4,4'-DDT used in this study

Property	Value
Purity	98.2%
Form	Powder
Molecular weight	354.49
Melting point	107–110 °C(L)
Flash point	72 °C

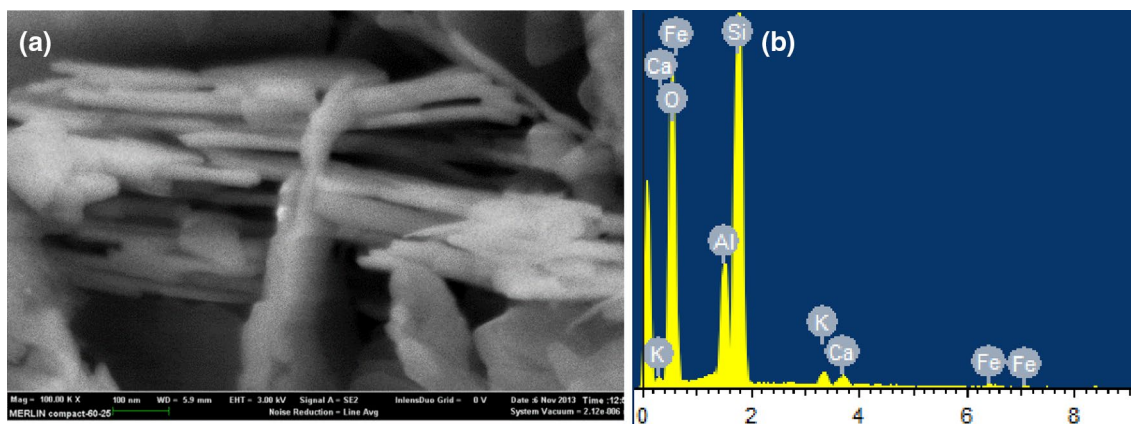


Fig. 1 Ferrierite zeolite particles: **a** SEM microscope photograph (plate-shaped appearance), **b** XRF results

Table 3 Properties of *n*-hexane

Property	Value
Molecular weight	86.18
Assay (%)	99.0
Density	0.66
Melting point (°C)	− 94.3
Boiling point (°C)	69 °C
Vapor pressure at 20 °C (hPa)	160
Explosion limits (%)	lower 1 vol.– upper 8.1 vol.
Residue on evaporation (%)	0.001 max.
Acidity (mEq./g.)	0.0005 max.
Water (%)	0.02 max.
Flash point (°C)	− 22
Sulfur compounds (%)	0.001 max.

Table 4 Some properties of soil used in this study

Property	Value
Moisture content (%)	20.7
pH at 20 °C	5.14
Organic carbon content (%)	5
Cation exchange capacity (meq/100 g)	10.9
Present clay fraction (< 2 μm)	29.6
Percent of gravel (%)	0.28
Percent of sand (%)	57.92
Percent of silt (%)	12.2
Liquid limit (%)	42.3
Plastic limit (%)	24.96
Plasticity index (%)	17.34
Specific gravity	2.7

soil classification system (USCS). Also, organic content by loss on ignition was done following ASTM D2974. Table 4 shows some properties of the soil. The cation exchange capacity (CEC) test had been accomplished following USEPA SW-846 method 9081. The method 9081 applies to most soils. Ten grams (10 g) of soil sample was mixed with an amount of sodium acetate solution, resulting in an exchange of the added sodium cations for the matrix cations. Subsequently, the sample was washed with isopropyl alcohol. An ammonium acetate solution was then added, which replaces the adsorbed sodium with ammonium. The process accomplished through series processes of shaking and centrifugation at the end ICP-MS then determines the concentration of displaced sodium.

Then, adsorption study of DDT on zeolite was conducted using batch adsorption test at different concentrations of DDT 5, 15, 30, and 50 ppm (mg/L). The quantity of zeolite used was 0.1, 0.5, 0.8, and 1.2 g in percentage around

0.833, 4.16, 6.66, and 10%, respectively. In batch adsorption test, a known volume of a solution of the test substance at a known concentrations and weight of zeolite was added to soil samples of known dry weight. The mixture was agitated for an appropriate time. Centrifugation and filtration then separated the soil suspensions, and the aqueous phase is analyzed using gas chromatography (GC). Results then analyzed using five adsorption kinetic models (pseudo-first-order kinetic model, pseudo-second-order kinetic model, intraparticle diffusion model, Elovich kinetic model, and Bangham kinetic model) and three equilibrium isotherm models (Freundlich, Langmuir, and Temkin). The effect of pH on the interaction of adsorption also investigated in this work at four different values of pH (3, 5, 7, and 9).

Batch adsorption test

DDT standard stock solution preparation Initially, stock solutions of 100 mg/L were prepared by dissolving 100 mg of DDT powder in 1 L (1000 mL) *n*-hexane (because DDT does not dissolve readily in water) in 1000-mL volumetric flask. Then standard solutions were prepared by diluting the stock to 5, 15, 30, and 50 mg/L with *n*-hexane. These standard solutions were then analyzed using gas chromatography (GC) to obtain the peak area for detection of the DDT and to calibrate GC before analyzing samples. Stock solutions were used to save preparation time, conserve materials, reduce storage space, and improve the accuracy of lower concentration solutions. Preferably, the stock solution was prepared directly before the application to soil samples. The solution must remain closed in the dark at 4 degrees Celsius (4 °C). Both the stability of the test substance and its concentration in the solution affect the storage time of the solution.

Adsorption equilibrium time determination All experiments were done at laboratory ambient temperature. Batch adsorption test was carried out following the OECD Guideline 106 (2000). The experiment was carried out using glass bottles, which can fit directly in the shaking or agitating device, to minimize handling and transfer errors. These bottles were capped to avoid volatility and losses. PTFE (Teflon)-lined screw caps were used to minimize adsorption on them. Soil/solution ratio selected was 1/5. Twelve grams (12 g) of soil were placed in each bottle and mixed with various amounts of nano-zeolite. Sixty milliliters (60 mL) of DDT solution was added to the soil and nano-zeolite mixture. Samples were shaken sequentially at 200 rpm (to keep the soil in suspension during shaking), over a 48-h period of mixing (1, 4, 10, 16, 24, 36, and 48 h). The mixture was shaken at constant temperature (28 °C) until adsorption equilibrium time was reached. After shaking, the samples were centrifuged in 50-mL centrifuge vials at 3000 rpm for 30 min. Centrifugation conditions should be capable to

remove particles with a diameter greater than 0.2 μm from aqueous solution. If the centrifugation facilities cannot guarantee the removal of particles larger than 0.2 μm , filtration with 0.2 μm filters could be used. Nylon syringe filters of 0.2 μm porosity, sole use was used for this purpose. Special attention should be taken to the selection of the filter material, to avoid losses of the test substance on it. Moreover, good care should be taken while filtering the samples. In all cases, it must be proved that no losses of the test substance occur during filtration.

The last step, filtered samples transferred to 1.5-mL glass vials (Fig. 2). Then all samples were analyzed by gas chromatography–electron capture detector (GC–ECD) analysis. The GC used was from Agilent model 7890A. All the experiments were performed in triplicate. All test tubes used in experiments were cleaned with distilled water and rinsed with acetone before use.

Determination the amount of adsorption The amount of DDT adsorbed onto zeolite surface was determined from the difference between the initial concentration of DDT present in solution and the amount remaining in the aqueous solution at the end of the experiment. The amount of adsorption of DDT at equilibrium (q_e) or at any time (q_t) was calculated in mg/kg from Eqs. 15 and 16 as follows:

$$q_t = (C_0 - C_t) \frac{v}{m} \quad (15)$$

$$q_e = (C_0 - C_e) \frac{v}{m} \quad (16)$$

where q_t and q_e are the amounts of DDT adsorbed onto zeolite surface at time t and at equilibrium. C_0 (mg/L) is the initial concentration of DDT solution, while C_t and C_e (mg/L) represent the final liquid phase concentration of DDT at time t and at equilibrium, v is the solution volume in mL, and m is the soil mass in g.

Effects of testing procedures on adsorption of DDT

For checking whether there is effect for the testing procedures on the adsorption process and considerably reduce



Fig. 2 Filtered samples in 1.5-mL glass vials before GC analysis

the concentration of DDT in the solution, blank samples were prepared. These blank samples contained only the DDT solution subjected to all steps of the testing that applied to the study samples. It is found there is no DDT lost during the procedure.

Effect of pH on Adsorption of DDT

The influence of pH on the adsorption of DDT was also studied. For this purpose, A 60 mL of DDT solution with different concentrations (5, 15, 30, and 50 mg/L) was added to test vials which contain 12 g of soil, and various amounts of zeolite were used. The pH value of the solution was adjusted using ammonia solutions (NH_3) with purity of 25% and acetic acid (CH_3COOH). Values of pH used in this study were 3, 5, 7, and 9. The content of vials was shaken (200 rpm) for 24 h at a constant temperature of 28 $^\circ\text{C}$. The solution was then centrifuged and filtered to separate the zeolite and soil particles. The residual concentration of DDT in the solution was measured by gas chromatography (GC). The amount of DDT adsorbed onto zeolite surface was determined by the difference between the initial and final concentration of DDT in the solution using Eqs. 15 and 16.

Result and discussion

The results of the experimental study of the adsorption of DDT onto different zeolite at various initial concentrations as a function of contact time were considered for determining the necessary equilibrium time. As the adsorption efficiency dominated by adsorption kinetics, the kinetic models such as pseudo-first-order kinetic model, pseudo-second-order kinetic model, intraparticle diffusion model, Elovich kinetic model, and Bangham kinetic model are commonly used for analysis of reaction process and mechanisms. These five models are widely used, assuming that maximum adsorption capacity occurs at equilibrium time when adsorbate covers the surface. The equilibrium isotherms are also very important for understanding the adsorption systems. Adsorption isotherm reflects the relationship between the amount of a solute adsorbed at constant temperature and its concentration in the equilibrium solution. There are several isotherm equations available for analyzing experimental adsorption equilibrium data. In this work, three adsorption isotherms Langmuir, Freundlich, and Temkin were applied to fit the equilibrium data of adsorption of DDT onto zeolite. Also, the effect of the pH value of the media on the adsorption of DDT onto zeolite at equilibrium time was also studied.

Adsorption of DDT onto zeolite surface

In this study, batch adsorption test was used to evaluate the application of zeolite to contaminated soil to remove DDT. The adsorption of DDT was studied in ambient conditions, and the initial pH value of (DDT+ soil) solutions recorded was 5.0. The initial concentrations of DDT solutions were 0,

5, 15, 30, and 50 ppm. The effect of the contact time on the removal of DDT is presented in Fig. 3a–e. All the experiments were conducted at room temperature. The adsorption uptake was found to increase with an increase in contact time and reaching equilibrium after about 24 h shaking time. This considered the appropriate time for maximum adsorption of DDT from the solution where after that time no more

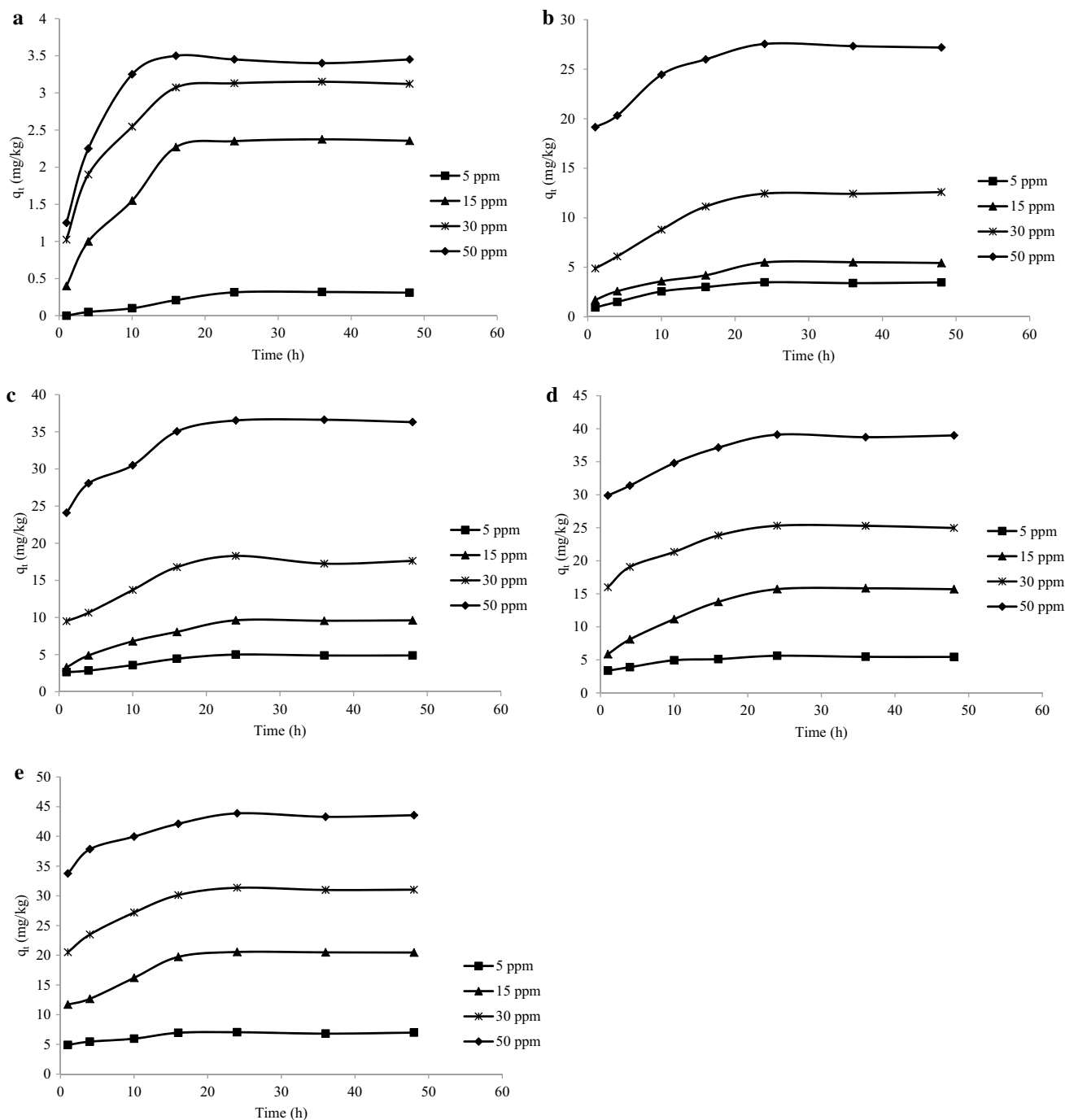


Fig. 3 Effect of shaking time on DDT adsorption onto zeolite at various initial concentrations **a** 0.0 g zeolite, **b** 0.1 g zeolite, **c** 0.5 g zeolite, **d** 0.8 g zeolite, and **e** 1.2 g zeolite

noticeable adsorption took place. At the equilibrium point, the amount of DDT desorbed from the liquid was in a state of dynamic equilibrium with the amount of DDT adsorbed on the zeolite. The amount of DDT adsorbed at the equilibrium time reflected the maximum adsorption uptake (overall adsorption < 30%) of the adsorbent.

Adsorption tests on the residual soil–DDT mixture are shown in Fig. 3a. A small limited adsorption was noted at all the initial concentrations of DDT, especially at 5 ppm. However, from Fig. 3b, for the addition of 0.1 g zeolite, the plot shows that the adsorption increases as shaking time increases up to 24 h and then no further increase in the adsorption amount. During this time, the adsorption uptake for 5, 15, 30, and 50 mg/L DDT was 3.478, 5.491, 12.48, and 27.55 mg/kg, respectively. It was reported that the remaining vacant surface sites are difficult to be occupied due to the formation of repulsion among DDT molecules (on the surface and in the bulk phase) [54]. These lead to a decrease in adsorption rate and exhibited by straight line after 24-h adsorption, reaching the steady-state condition [55].

Similar adsorption trends were observed at 0.5, 0.8, and 1.2 g zeolite content as shown in Fig. 3c–e, respectively. However, the amount of adsorption increased as zeolite content increased. For 0.5 g zeolite content, the amount of adsorption was 5.491, 9.622, 18.288, and 36.526 mg/kg for 5, 15, 30, and 50 mg/L initial concentration of DDT, respectively. Further increase in zeolite content to 0.8 g increased the adsorption to 5.62, 15.71, 25.32, and 39.105 mg/kg for 5, 15, 30, and 50 mg/L initial concentration of DDT, respectively. Maximum adsorption occurred at 1.2 g zeolite content, which was 7.045, 36.526, 20.55, and 43.875 mg/kg for 5, 15, 30, and 50 mg/L initial concentration of DDT, respectively.

All the results show that the percentage of absorption increases with the increase in zeolite dosage. Therefore, the maximum adsorption was observed to be at the highest level of zeolite due to the maximum capacity of adsorption sites. The maximum percentage of adsorption for the parameters obtained from this study is 28.20%. The study of the influence of adsorbent dose on the removal of DDT from soil solution has significant importance in economic terms. The results also show that the rate of the adsorption decreased with time. This is because at the beginning of the tests all adsorption sites are empty, and adsorbed substance is easily replaced in the empty sites. With the passage of time, the empty zeolite sites decreased, and the rate of adsorption decreased also. About 30% of the total adsorption happened during the first hour, and more than 50% happened in less than 10 h, and after 24 h, the rate of the adsorption was almost insignificant. Figure 3 shows that after 24 h, the experimental line was nearly horizontal, indicating that no further adsorption took place.

Accordingly, all the adsorption kinetic models and equilibrium isotherm models in “Data fitting to model equations” section were studied at a contact time of 24 h to ensure equilibrium adsorption.

Data fitting to model equations

Adsorption mechanism and kinetics

Pseudo-first-order model To identify the key process controlling the adsorption rate, several models were checked for suitability and consistency over a broad range of the system parameters. Figure 4 shows data fitting to pseudo-first-order kinetic model. The plots of $\ln(q_e - q_t)$ against t at 0.1, 0.5, 0.8, and 1.2 g zeolite content are shown in Fig. 4a–d, respectively. The values of $\ln(q_e - q_t)$ at 0.1, 0.5, 0.8, and 1.2 g zeolite content are calculated from the experimental data. Fitting kinetic parameters of adsorption of DDT on zeolite according to pseudo-first-order model (Eq. 2) at 0.1, 0.5, 0.8, and 1.2 g zeolite content are tabulated in Table 5. From Fig. 4, the results show that the values of $\ln(q_e - q_t)$ with adsorption time are far apart and the values were nonlinear. As noted by the results, the values in the axis of time were limited to 16 h; the reason is that the values of $\ln(q_e - q_t)$ is equal to zero at time 24 h; therefore, the result will be infinity or undefined.

Acceptable R^2 values were noted, but there are some notable variances between the experimental and theoretical uptakes as shown in Table 5. However, pseudo-first-order model shows accepted data fitting. Thus, the pseudo-first-order model can be applicable for the adsorption of DDT on zeolite, and the adsorption of DDT on zeolite is not first-order reaction.

Pseudo-second-order kinetic model The values of $\frac{t}{q_t}$ are plotted against t as shown in Fig. 5. Kinetic parameters of adsorption of DDT onto zeolite according to pseudo-second-order model (Eq. 4) at 0.1, 0.5, 0.8, and 1.2 g zeolite content are tabulated in Table 6. Figure 5 shows that the experimental data are well simulated and the plots for the values of $\frac{t}{q_t}$ with adsorption time are linear, especially for high concentrations of DDT (30 and 50 ppm). The results show that pseudo-second-order model fits the experimental data quite well and the R^2 values reached the unity indicating experimental and theoretical uptakes are in good agreement. This indicates the applicability of the second-order kinetic model to describe the adsorption process of DDT onto zeolite.

Intraparticle diffusion model The curve-fitting plots of the intraparticle diffusion model of adsorption of DDT onto zeolite at 0.1, 0.5, 0.8, and 1.2 g zeolite content are demon-

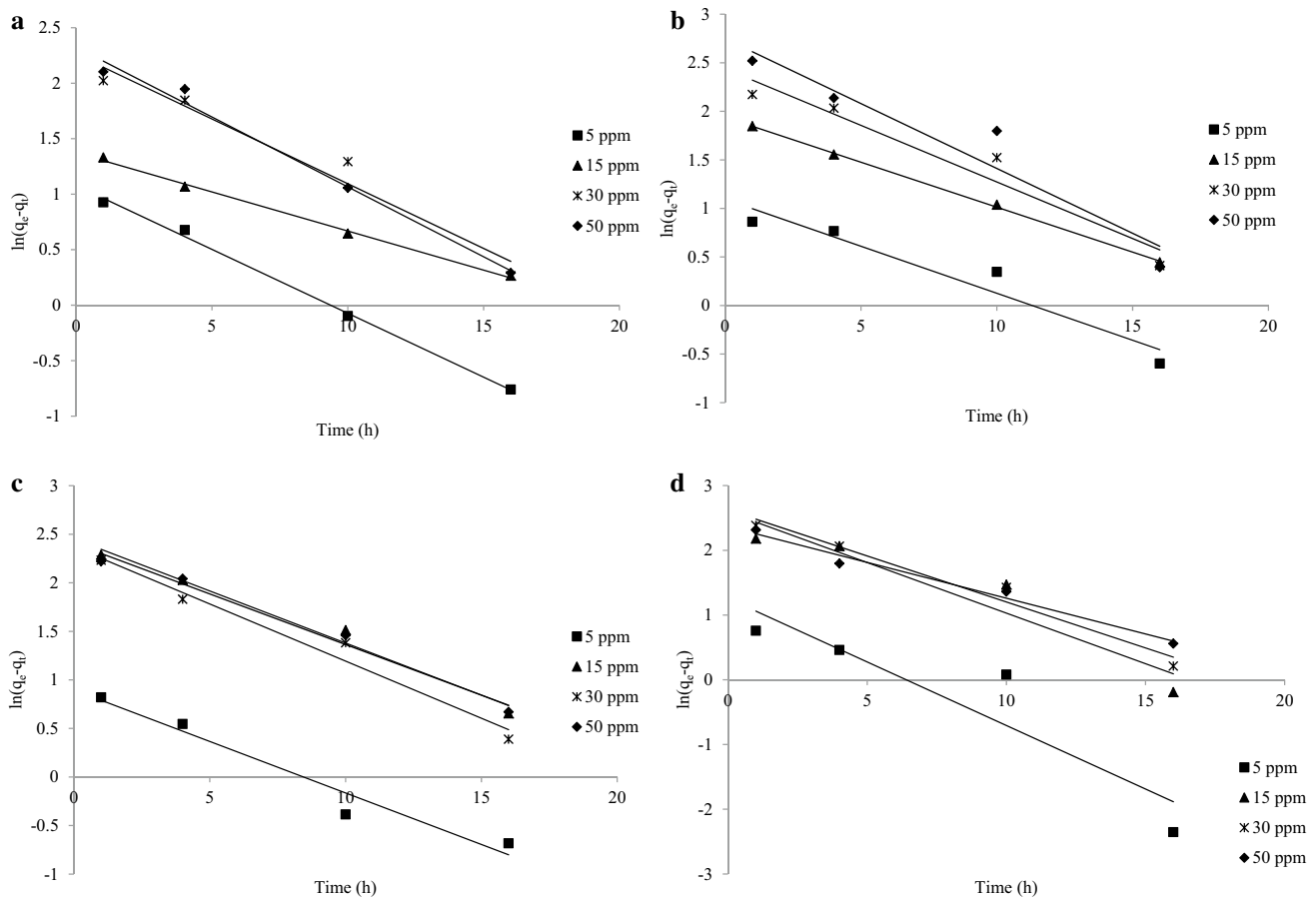


Fig. 4 Plots of $\ln(q_e - q_t)$ versus time (h) for adsorption of DDT onto zeolite. The solid points belong to experimental data, while the line is calculated from nonlinear least square regression of the data accord-

ing to pseudo-first-order rate expression (Eq. 2), **a** 0.1 g zeolite, **b** 0.5 g zeolite, **c** 0.8 g zeolite, and **d** 1.2 g zeolite

Table 5 Fitting kinetic parameters of adsorption of DDT onto zeolite according to pseudo-first-order model (Eq. 2) at 0.1, 0.5, 0.8, and 1.2 g zeolite content

Zeolite content (g)	C_0 (mg/L)	$q_{e,exp}$ (mg/kg)	$q_{e,cal}$ (mg/kg)	k_1 (1/h)	R^2
0.1	05 ppm	3.4666	2.93997	0.1151	0.9969
	15 ppm	5.490925	3.94520	0.0704	0.9965
	30 ppm	12.438	9.58979	0.1166	0.9608
	50 ppm	27.3275	10.22974	0.1259	0.988
0.5	05 ppm	5.0041	2.98679	0.0968	0.9321
	15 ppm	9.6220	6.95040	0.0926	0.9992
	30 ppm	18.2875	11.45928	0.1166	0.9401
	50 ppm	36.5260	15.59733	0.1336	0.9183
0.8	05 ppm	5.6200	2.45027	0.1061	0.9558
	15 ppm	15.7088	11.61503	0.1073	0.9822
	30 ppm	25.3200	10.69739	0.1176	0.9734
	50 ppm	39.1050	11.08729	0.1042	0.9842
1.2	05 ppm	7.0450	3.51626	0.1964	0.8459
	15 ppm	20.5500	13.34444	0.1562	0.9025
	30 ppm	31.3560	13.77423	0.1421	0.9714
	50 ppm	43.8750	10.64403	0.1106	0.981

strated in Fig. 6. However, if intraparticle diffusion occurs, then q_t versus $t^{1/2}$ will be linear and if the plot passes through the origin, then the rate limiting process is only due to the intraparticle diffusion. Otherwise, some other mechanism along with intraparticle diffusion is also involved.

The values of k_3 and C_i obtained from the plots at 0.1, 0.5, 0.8, and 1.2 g (Table 7) indicate that the intraparticle diffusion model is not applicable. Since the plots of q_t versus $t^{1/2}$ (Fig. 6) do not pass through zero and most of values of the coefficient correlation (R^2) are less 0.9 (Table 7), the intraparticle diffusion is not the rate-controlling step of the adsorption mechanism for the adsorption of DDT onto zeolite surface.

Elovich kinetic model Figure 7 shows the curve-fitting plots of the Elovich kinetic model of adsorption of DDT onto zeolite at 0.1, 0.5, 0.8, and 1.2 g zeolite content. The values of α and β obtained from the plots at 0.1, 0.5, 0.8, and 1.2 g are demonstrated in Table 8.

The result shows that although a linear relationship existed, the overall line was not straight. Despite the almost

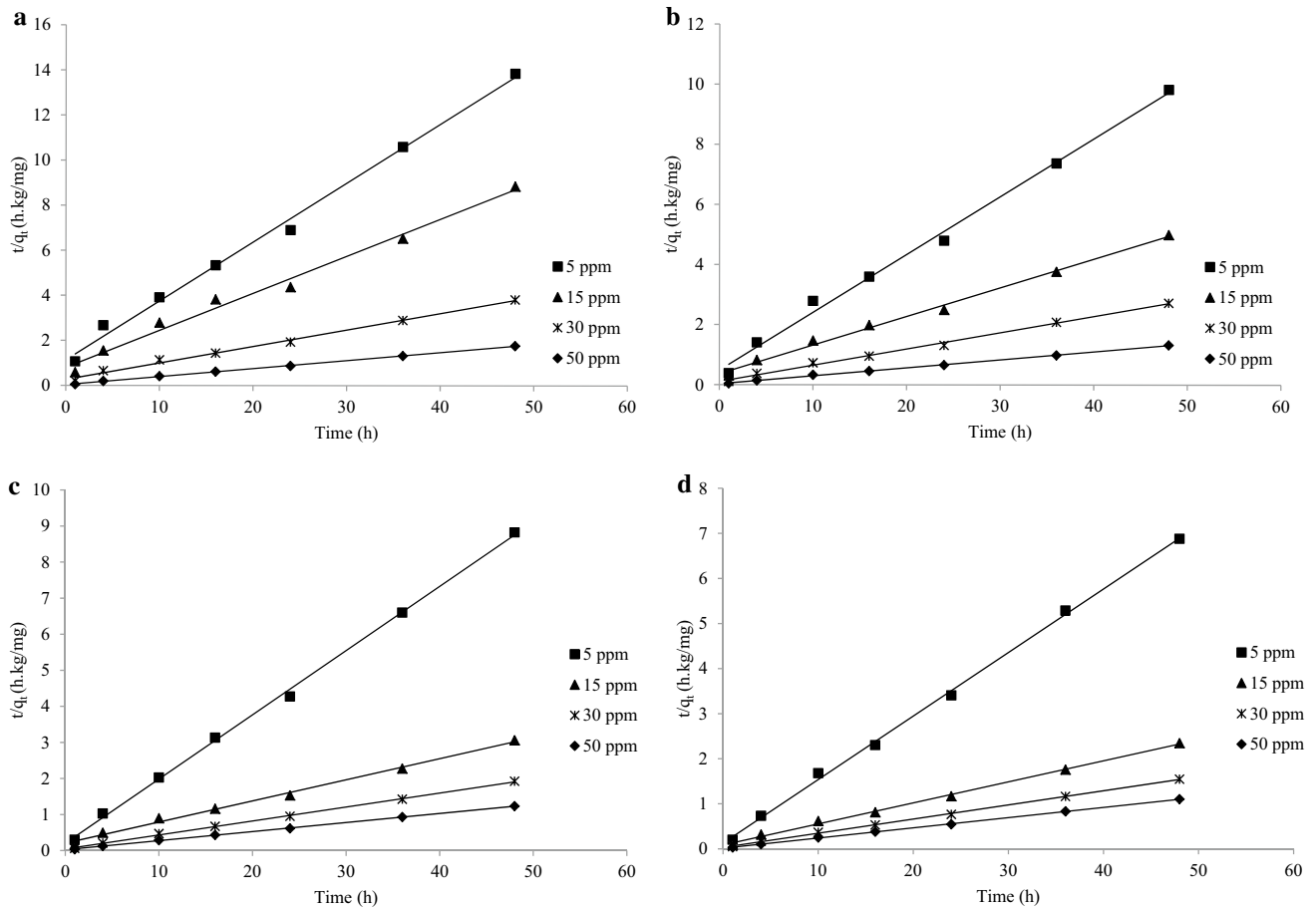


Fig. 5 Plots of $\frac{t}{q_t}$ versus time (h) for adsorption of DDT onto zeolite. The solid points belong to experimental data, while the line is calculated from nonlinear least square regression of the data according to

pseudo-second-order rate expression (Eq. 4), **a** 0.1 g zeolite, **b** 0.5 g zeolite, **c** 0.8 g zeolite, and **d** 1.2 g zeolite

Table 6 Fitting kinetic parameters of adsorption of DDT onto zeolite according to pseudo-second-order kinetic model (Eq. 4) at 0.1, 0.5, 0.8, and 1.2 g zeolite content

Zeolite content (g)	C_0 (mg/L)	$q_{e,exp}$ (mg/kg)	$q_{e,cal}$ (mg/kg)	k_2 (kg/mg h)	R^2
0.1	05 ppm	3.4666	3.82409	0.0601638	0.9946
	15 ppm	5.490925	6.07533	0.0338453	0.9873
	30 ppm	12.438	13.64256	0.0198922	0.9942
	50 ppm	27.3275	27.93296	0.0357003	0.9992
0.5	05 ppm	5.0041	5.192108	0.0766896	0.9946
	15 ppm	9.6220	10.4712042	0.024911909	0.9945
	30 ppm	18.2875	18.4501845	0.027326883	0.9956
	50 ppm	36.5260	37.45318352	0.022776038	0.9988
0.8	05 ppm	5.6200	5.61482313	0.15671744	0.9987
	15 ppm	15.7088	17.0940171	0.016620932	0.9946
	30 ppm	25.3200	25.8397933	0.032629411	0.9988
	50 ppm	39.1050	39.68253968	0.029130275	0.9995
1.2	05 ppm	7.0450	7.097232079	0.155221344	0.9986
	15 ppm	20.5500	21.45922747	0.024482074	0.9973
	30 ppm	31.3560	31.84713376	0.030244171	0.9993
	50 ppm	43.8750	44.05286344	0.037612408	0.9997

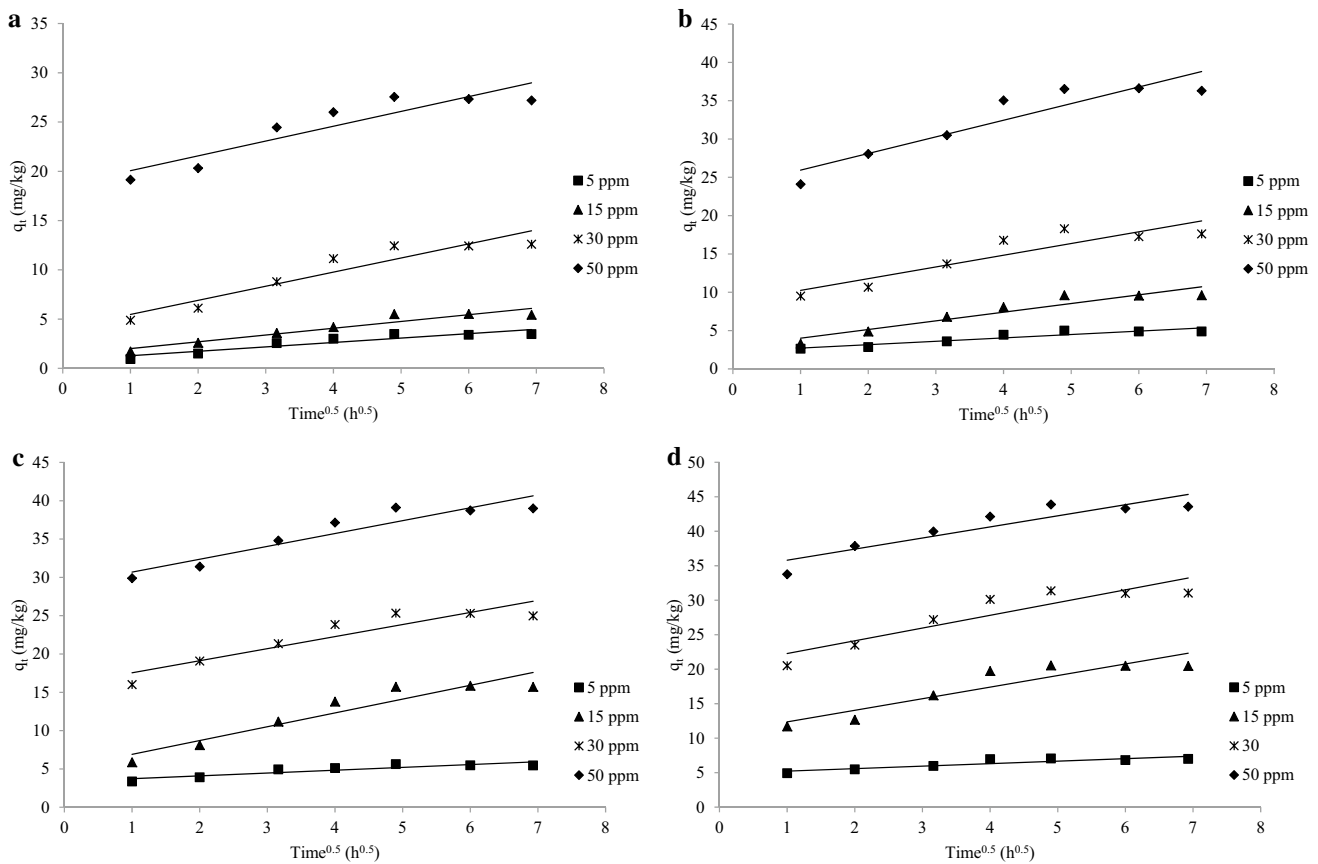


Fig. 6 Intraparticle diffusion plots for the adsorption of DDT (Eq. 5) onto zeolite at **a** 0.1 g zeolite, **b** 0.5 g zeolite, **c** 0.8 g zeolite, and **d** 1.2 g zeolite

Table 7 Fitting kinetic parameters of adsorption of DDT onto zeolite according to intraparticle diffusion model (Eq. 5) at 0.1, 0.5, 0.8, and 1.2 g zeolite content

Zeolite content (g)	C_0 (mg/L)	C_i	k_3 (kg/mg h ^{0.5})	R^2
0.1	05 ppm	0.829	0.4481	0.8658
	15 ppm	1.3233	0.6873	0.9143
	30 ppm	4.0399	1.4319	0.8916
	50 ppm	18.55	1.5046	0.8409
0.5	05 ppm	2.267	0.4438	0.8694
	15 ppm	2.874	1.1327	0.901
	30 ppm	8.7129	1.529	0.8272
	50 ppm	23.771	2.1698	0.8588
0.8	05 ppm	3.3591	0.3681	0.8071
	15 ppm	5.1125	1.8001	0.8932
	30 ppm	15.964	1.5761	0.8558
	50 ppm	29.001	1.6812	0.8825
1.2	05 ppm	4.8568	0.3617	0.7989
	15 ppm	10.678	1.6811	0.8457
	30 ppm	20.422	1.8481	0.835
	50 ppm	34.2	1.6093	0.8358

good values of correlation coefficients (R^2 , Table 8), it is clear that a simple Elovich equation is not the best model to express adsorption of DDT onto the surface of the zeolite. Thus, the Elovich kinetic model cannot describe the kinetics of adsorption of DDT onto zeolite surface.

Bangham kinetic model Figure 8 presents the results of fitting experimental data to the Bangham kinetic model of adsorption of DDT onto zeolite at 0.1, 0.5, 0.8, and 1.2 g zeolite content. Table 9 lists the kinetic constants obtained from the Bangham equation for the plots at 0.1, 0.5, 0.8, and 1.2 g zeolite content. If Bangham equation represents the experimental data, then the adsorption kinetics is limited by the pore diffusion [50].

The result in Table 9 shows that the value of rate constant for adsorption (k_i) increases with the increase in the initial concentration of DDT. At 1.2 g zeolite content, k_i values were 4.88955 and 34.16152 for 5 and 50 mg/L of DDT initial concentration, respectively. In addition, results show relatively high values of correlation coefficients (R^2 , Table 9). The values of the correlation coefficients for the pseudo-second-order kinetic model are higher than those

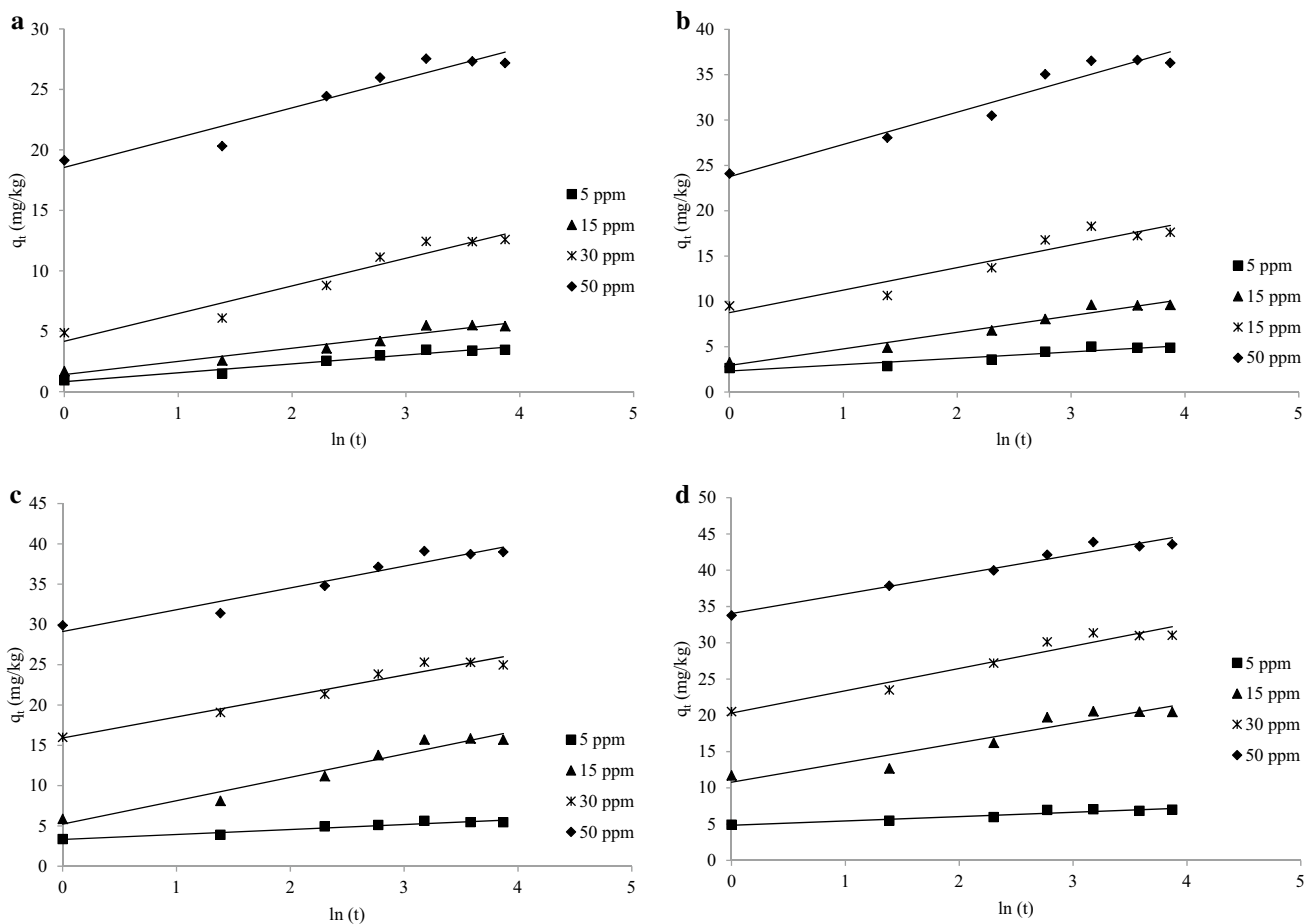


Fig. 7 Plots of q_t versus $\ln(t)$ for adsorption of DDT onto zeolite. The solid points belong to experimental data, while the line is calculated from nonlinear least square regression of the data according to

Elovich kinetic model (Eq. 7), **a** 0.1 g zeolite, **b** 0.5 g zeolite, **c** 0.8 g zeolite, and **d** 1.2 g zeolite

Table 8 Fitting kinetic parameters of adsorption of DDT onto zeolite according to Elovich kinetic model (Eq. 7) at 0.1, 0.5, 0.8, and 1.2 g zeolite content

Zeolite content (g)	C_0 (mg/L)	β	α (mg kg ⁻¹ min ⁻¹⁵)	$q_{e,exp}$ (mg/kg)	$q_{e,cal}$ (mg/kg)	R^2
0.1	05 ppm	1.3618	2.2658	3.4666	3.1611	0.9525
	15 ppm	0.9181	3.9810	5.4909	4.8732	0.9405
	30 ppm	0.4364	14.136	12.438	11.4523	0.9353
	50 ppm	0.4061	4612.8	27.328	26.379	0.9224
0.5	05 ppm	1.4263	19.441	5.0041	4.5575	0.8888
	15 ppm	0.5472	9.1338	9.6220	8.7484	0.9606
	30 ppm	0.4031	85.015	18.288	16.6524	0.8921
	50 ppm	0.2814	2851.5	36.526	35.0634	0.9438
0.8	05 ppm	1.6197	134.33	5.6200	5.2853	0.93
	15 ppm	0.34446	17.528	15.7088	14.446	0.9517
	30 ppm	0.384	1169.5	25.3200	24.1832	0.9573
	50 ppm	0.3698	128628	39.1050	37.713	0.9351
1.2	05 ppm	1.673	1973.1	7.0450	6.7432	0.8937
	15 ppm	0.3690	144.93	20.5500	19.3946	0.9
	30 ppm	0.3254	2276.6	31.3560	30.073	0.9457
	50 ppm	0.37056	812,736	43.8750	42.6203	0.9627

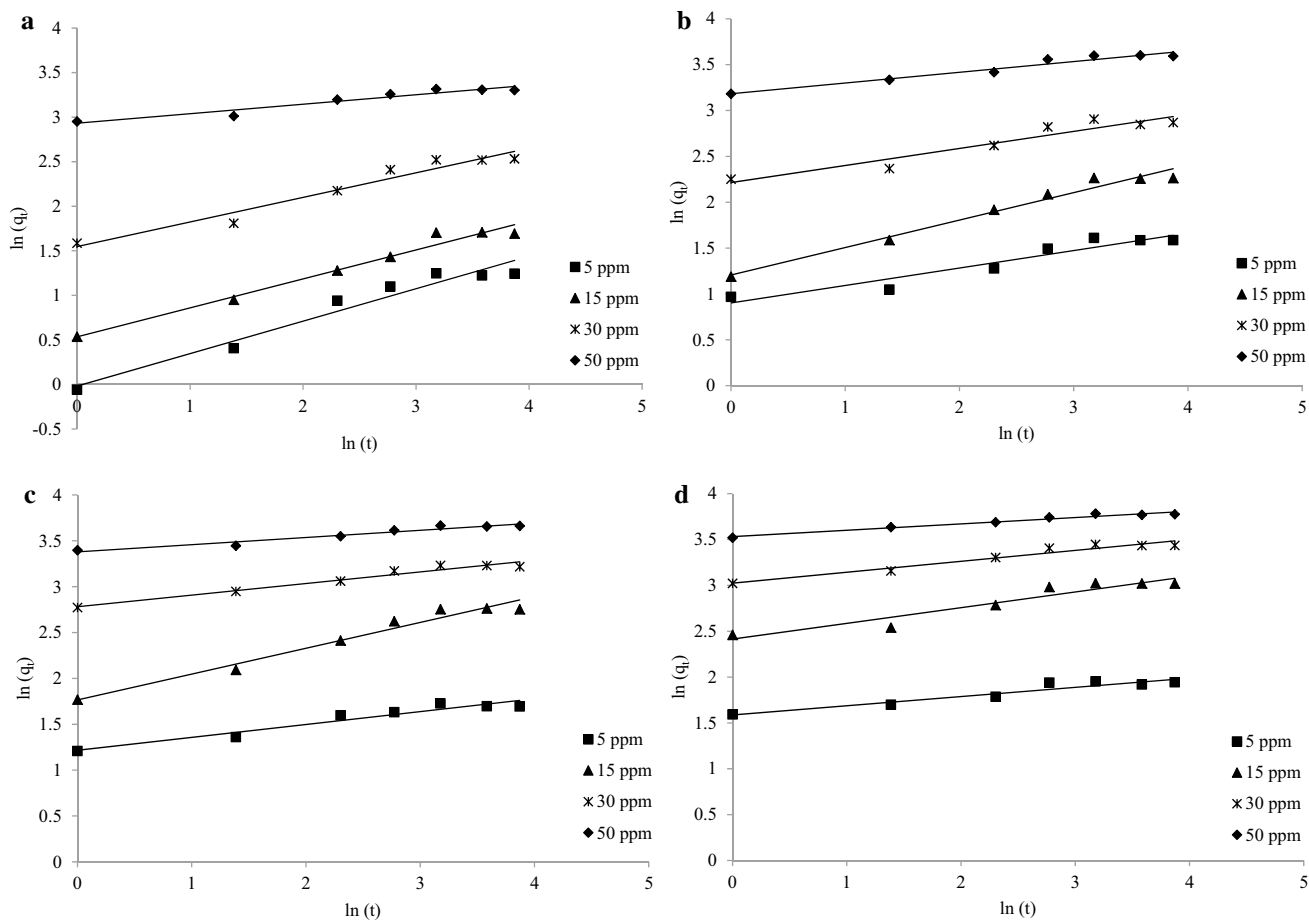


Fig. 8 Plots of $\ln(q_t)$ versus $\ln(t)$ for adsorption of DDT onto zeolite. The solid points belong to experimental data, while the line is calculated from nonlinear least square regression of the data according to Bangham kinetic model (Eq. 9), **a** 0.1 g zeolite, **b** 0.5 g zeolite, **c** 0.8 g zeolite, and **d** 1.2 g zeolite

Table 9 Fitting kinetic parameters of adsorption of DDT onto zeolite according to Bangham kinetic model (Eq. 9) at 0.1, 0.5, 0.8, and 1.2 g zeolite content

Zeolite content (g)	C_0 (mg/L)	k_t	m	$q_{e,exp}$ (mg/kg)	$q_{e,cal}$ (mg/kg)	R^2
0.1	05 ppm	0.98137	2.745	3.4666	3.12364	0.9536
	15 ppm	1.706	3.076	5.4909	4.79314	0.9751
	30 ppm	4.6974	3.6206	12.438	11.3	0.9525
	50 ppm	18.771	9.3985	27.328	26.323	0.9252
0.5	05 ppm	2.465	5.2576	5.0041	4.512	0.9094
	15 ppm	3.34076	3.3389	9.6220	8.6540	0.9738
	30 ppm	9.155	5.3792	18.288	16.5287	0.9119
	50 ppm	24.11	8.5324	36.526	34.9902	0.9525
0.8	05 ppm	3.3754	7.1225	5.6200	5.2735	0.9332
	15 ppm	5.848	3.5574	15.7088	14.2884	0.9676
	30 ppm	16.14645	7.9114	25.3200	24.1288	0.962
	50 ppm	29.3355	12.723	39.1050	37.6599	0.9411
1.2	05 ppm	4.88955	9.9502	7.0450	6.7294	0.9083
	15 ppm	11.1920	5.8514	20.5500	19.2658	0.9113
	30 ppm	20.5632	8.40336	31.3560	30.015	0.9498
	50 ppm	34.16152	14.3885	43.8750	42.6051	0.9614

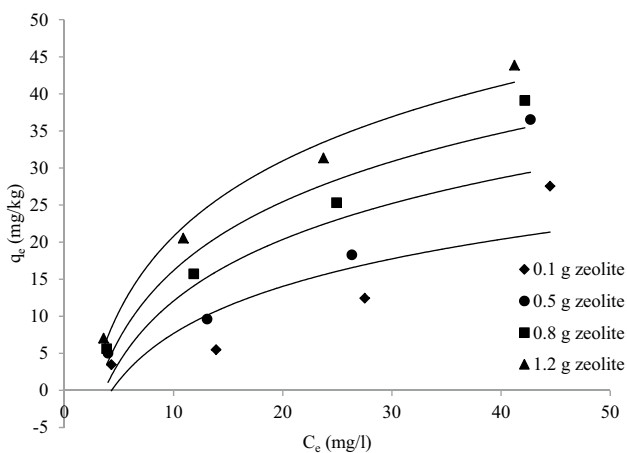


Fig. 9 Adsorption isotherms for DDT onto zeolite

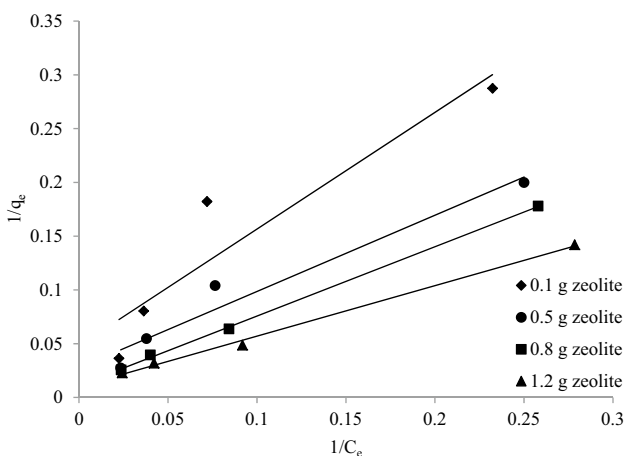


Fig. 10 Langmuir isotherm model for the adsorption of DDT on zeolite

obtained for Bangham model. This result still confirmed that the pore diffusion is not the only rate-controlling step.

Adsorption isotherms

The equilibrium isotherms are very important for understanding the adsorption systems. As shown in Fig. 9, the adsorption isotherms at various concentrations of DDT are nonlinear. Figure 9 illustrates that adsorption of DDT increase when the amount of zeolite increased. In addition, the results show that at C_e higher than 10 mg/L and for higher zeolite content (0.8 and 1.2), the plot can be approximated by a linear or a straight-line graph. This means that adsorption is directly proportional to the amount of DDT available at high concentrations of DDT and zeolite content.

Langmuir isotherm Figure 10 shows experimental data fitted for DDT on zeolite in linearized Langmuir model. Val-

Table 10 Langmuir, Freundlich, and Temkin parameters of adsorption isotherms of DDT onto zeolite (according to Eqs. 11, 13, and 14)

Model	Parameters	Zeolite content			
		0.1	0.5	0.8	1.2
Langmuir	k_1	0.04432	0.03907	0.01736	0.02127
	q_{max}	20.79	36.10	89.285	100
	R^2	0.8764	0.9538	0.9993	0.9969
Freundlich	K_f	0.8179	1.4462	1.9717	2.9686
	n	1.168	1.2335	1.245	1.3443
	R^2	0.9016	0.9554	0.9948	0.98
Temkin	a	-13.414	-15.5	-14.639	-13.001
	b	9.159	11.966	13.377	14.67
	R^2	0.7246	0.7825	0.9426	0.9815

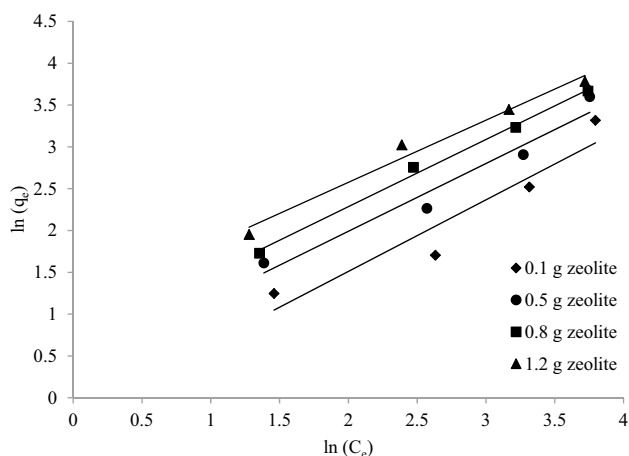


Fig. 11 Freundlich Isotherm model for the adsorption of DDT on zeolite

ues of k_1 and q_{max} are 0.04432 and 20.79 at 0.1 g of zeolite, while k_1 and q_{max} become 0.02127 and 100 at 1.2 g of zeolite, respectively. k_1 is the Langmuir constant and q_{max} is maximum adsorption capacity, which is related to the amount of adsorbate adsorbed at monolayer coverage. Determination coefficient (R^2) of values between 0.8764 and 0.9969 given in Table 10 indicates almost good correlation coefficient for Langmuir isotherm [56]. The means that the Langmuir isotherm fits well the adsorption data and may be can applicable for adsorption of DDT on zeolite but still not the best model which can express the adsorption reaction between DDT and zeolite due to low correlation coefficient (R^2) at 0.1 g zeolite content.

Freundlich isotherm Figure 11 shows experimental data fitted for DDT on zeolite in linearized Freundlich isotherm model. Table 10 lists Freundlich isotherm parameters for the plots at 0.1, 0.5, 0.8, and 1.2 g zeolite content. As observed, the value of k_f increases with increasing amount of zeolite.

k_f is Freundlich constant indicative of the relative adsorption capacity of the adsorbent. The result in Table 10 shows that the value of n is greater than 1 and also increases with the increasing amount of zeolite. The constant n is the Freundlich equation exponent that represents the parameter characterizing quasi-Gaussian energetic heterogeneity of the adsorption surface. It is generally stated that values of n in the range 2–10 represent good, 1–2 moderately difficult, and less than 1 poor adsorption characteristics [57]. Thus, a moderate adsorption characteristic occurred for DDT on zeolite. At 1.2 g zeolite content, the k_f parameter is 2.9686 and correlation coefficient, R^2 is 0.98, which indicates a good adsorption.

Temkin isotherm Temkin isotherm model experimental data fitted for DDT on zeolite are shown in Fig. 12. Also,

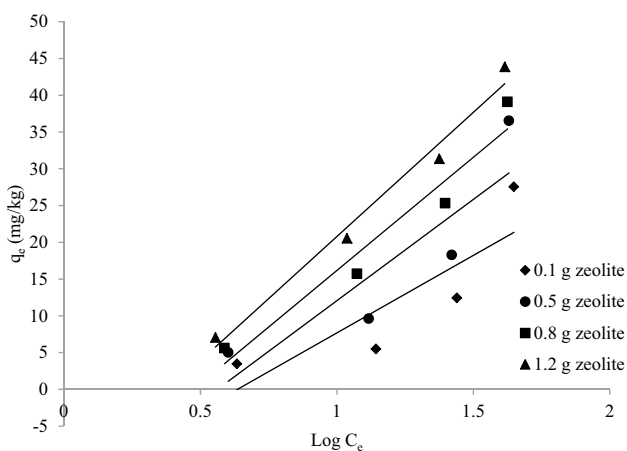


Fig. 12 Temkin Isotherm model for the adsorption of DDT on zeolite

Table 10 lists Temkin isotherm parameters for the plots at 0.1, 0.5, 0.8, and 1.2 g zeolite content. The Temkin isotherm model contains a factor that explicitly considers the adsorbent–adsorbate interactions. The results listed in Table 10 show negative values for equilibrium binding constant (a) and values for correlation coefficient (R^2) far apart from unity at low amounts of zeolite, which indicates a weak interaction between adsorbate and adsorbent for the present model. Despite the high values for correlation coefficient (R^2) at high zeolite content, R^2 is 0.9815 at 1.2 g, and the Temkin isotherm model is not very applicable to express the adsorption of DDT onto zeolite surface.

Models comparison

To understand the adsorption systems and check for suitability and consistency over a broad range of the system parameters, several kinetic models and adsorption isotherm models have been used. Five kinetic models and three adsorption isotherm equations are used in this study to analyze the adsorption experimental data. However, Table 11 shows a comparison between the five kinetic models at different contents of zeolite. The results showed that the highest correlation coefficient (R^2) values were noted for pseudo-second-order and Bangham kinetic models. The correlation coefficient R^2 is closest to 1 for pseudo-second-order model which indicates that the pseudo-second-order model is most suitable for describing the adsorption kinetics of DDT on the zeolite. In general, R^2 varies in the order: pseudo-second-order > Bangham > pseudo-first-order model > Elovich > intraparticle diffusion model.

Table 11 Correlation coefficient models comparison

Zeolite content (g)	C_0 (mg/L)	R^2				
		Pseudo-first-order	Pseudo-second-order	Intraparticle diffusion	Elovich kinetic	Bangham kinetic
0.1	05 ppm	0.9969	0.9946	0.8658	0.9525	0.9536
	15 ppm	0.9965	0.9873	0.9143	0.9405	0.9751
	30 ppm	0.9608	0.9942	0.8916	0.9353	0.9525
	50 ppm	0.988	0.9992	0.8409	0.9224	0.9252
0.5	05 ppm	0.9321	0.9946	0.8694	0.8888	0.9094
	15 ppm	0.9992	0.9945	0.901	0.9606	0.9738
	30 ppm	0.9401	0.9956	0.8272	0.8921	0.9119
	50 ppm	0.9183	0.9988	0.8588	0.9438	0.9525
0.8	05 ppm	0.9558	0.9987	0.8071	0.93	0.9332
	15 ppm	0.9822	0.9946	0.8932	0.9517	0.9676
	30 ppm	0.9734	0.9988	0.8558	0.9573	0.962
	50 ppm	0.9842	0.9995	0.8825	0.9351	0.9411
1.2	05 ppm	0.8459	0.9986	0.7989	0.8937	0.9083
	15 ppm	0.9025	0.9973	0.8457	0.9	0.9113
	30 ppm	0.9714	0.9993	0.835	0.9457	0.9498
	50 ppm	0.981	0.9997	0.8358	0.9627	0.9614

For the isotherm models (Table 10), the results of R^2 show that Freundlich isotherm model fits experimental data better than Langmuir model at 0.1 and 0.5 g zeolite content, but Langmuir fits better at 0.8 and 1.2 g zeolite content. The comparison table shows high correlation coefficient (R^2) for Temkin model at high zeolite content (at 0.8 and 1.2, R^2 values were 0.9426 and 0.9815, respectively), but the values were relatively low at lower amounts of zeolite (at 0.1 and 0.5, R^2 values were 0.7246 and 0.7825, respectively). Thus, the Langmuir and Freundlich isotherms are more suitable than Temkin to describe the adsorption equilibrium of DDT onto zeolite.

Effect of solution pH

The influence of pH on adsorption is complex and potentially could have a significant effect on the results of experiments. The variation in pH can result in a change in chemical speciation, consequently altering their adsorption characteristics [58]. In this research, the effect of pH on the adsorption of DDT from the contaminated soil onto

zeolite surface was investigated. The adsorption of DDT was significantly influenced by the pH values of the solution, which affects the surface charge of adsorbent and the degree of ionization as well as the speciation of solute. Therefore, the adsorption pattern of DDT on zeolite was studied at a variety of solution pH values from 3 to 9. Figure 13 and Table 12 show the adsorption of DDT, q_e (mg/kg), onto zeolite versus the solution pH at the initial concentrations (05–50 mg/L) after 24 h shaking time.

As illustrated in Fig. 13, the amount of DDT uptake on the zeolite surface was found to decrease with increasing pH of the solution for all initial concentration and for all zeolite contents, where the maximum uptake was noted at pH 3. The adsorption was highest for the solution of pH 5 and continuously until pH 9 where the poorest adsorption achieved. The highest rate of adsorption achieved at pH 3 was 30.68% at 1.2 g zeolite content, while it decreases until it reaches 2% at some samples for 0.1 g of zeolite.

In general, increases in pH lead to increased ionization, solubility, and hydrophilicity, and thus decreased adsorption of natural organic matter, resorcinol, and herbicides

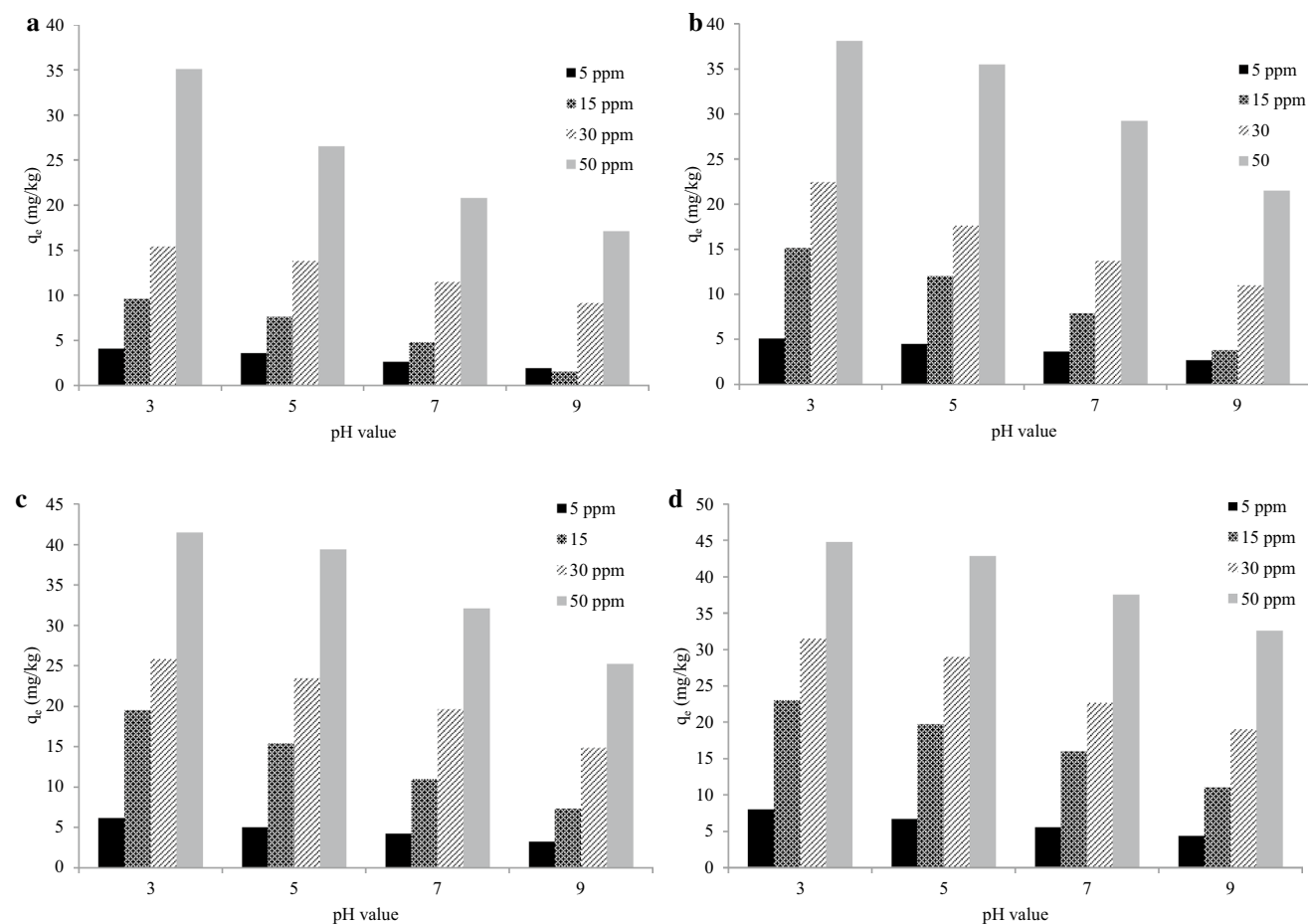


Fig. 13 Effect of solution pH for adsorption of DDT onto zeolite at various initial concentrations **a** 0.1 g zeolite, **b** 0.5 g zeolite, **c** 0.8 g zeolite, and **d** 1.2 g zeolite

Table 12 Effect of solution pH on adsorption capacity

Zeolite content (g)	pH value	Initial concentration C_0 (mg/L)			
		05	15	30	50
		q_e (mg/kg)			
0.1	3	4.1	9.59	15.4	35.067
	5	3.6	7.6	13.815	26.5
	7	2.652	4.816	11.46	20.75
	9	1.913	1.539	9.12	17.1
0.5	3	5.1	15.137	22.45	38.07
	5	4.495	12	17.61	35.5
	7	3.623	7.9	13.717	29.2
	9	2.716	3.765	11	21.48
0.8	3	6.15	19.516	25.8	41.45
	5	5.01	15.4	23.442	39.4
	7	4.229	10.985	19.635	32.05
	9	3.271	7.296	14.826	25.2
1.2	3	8.001	23.006	31.45	44.755
	5	6.68	19.7	29	42.85
	7	5.518	16	22.619	37.55
	9	4.381	11.046	18.993	32.55

[58]. In other words, the removal efficiency of DDT increases in acidic solution due to the natural decomposition at lower pH [59]. Therefore, the analysis carried out in this study demonstrated that increasing pH value resulted in diminishing adsorption capacity. Therefore, the result of remediation soil-DDT with different pH shows the importance of working in the acid medium. Poursaberi et al. [60] compared the removal efficiencies of DDT by nanoscale zero-valent iron (NZVI), for pH 9 and pH 2. The results showed 99.2% removal of DDT after a treatment time of 240 min for pH 2, while for pH 9 it had 26% removal efficiency. However, Gholikandi et al. [30] found that the removal efficiency of heavy metals by natural zeolite increased as pH value decreased in the water sample.

Conclusions

In this work, batch adsorption test was conducted at different initial concentrations of DDT (5, 15, 30 and 50 mg/L) and with 0.1, 0.5, 0.8, and 1.2 g zeolite content. The adsorption models were examined by five different kinetic models (the pseudo-first-order kinetic model, the pseudo-second-order kinetic model, intraparticle diffusion model, Elovich kinetic model, and Bangham kinetic model) and three equilibrium isotherm models (Freundlich, Langmuir, and Temkin). The effect of pH on the interaction of adsorption was also investigated in this work at four

different values of pH (3, 5, 7, and 9). From the results of this study, the following conclusions can be drawn:

1. The zeolite has a moderate adsorption capacity for the DDT. The highest adsorption capacity obtained from the adsorption of the DDT on to the zeolite surface was about 28.20%. Also, the result shows that DDT concentration in soil samples decreases significantly with the increase in the amount of the zeolite, and the maximum adsorption was conducted at 1.2 g zeolite.
2. In the application of adsorption kinetics, the comparison of R^2 values indicates that all five kinetics fitted the experimental data well. The result also shows the best agreement model with experimental data is the pseudo-second-order model.
3. The comparison of R^2 values indicates that both Langmuir and Freundlich isotherm models fit experimental data better than Temkin isotherm equations where the determination correlation coefficients (R^2) of Temkin equations are relatively low, and correlation coefficients (R^2) of Langmuir and Freundlich equations are much higher. Thus, the Langmuir and Freundlich isotherms are both suitable equations to describe the adsorption equilibrium of DDT onto zeolite.
4. The effectiveness of treatment process can highly affect the value of pH. Results show that the increase in pH has a negative effect on the adsorption process, and the amount of DDT uptake on the zeolite surface was found to decrease with increasing pH of the solution for all initial concentration at all zeolite content. However, acidic media have a significant effect on the adsorption interaction, and the maximum uptake of DDT was noted at pH 3. Therefore, the result of remediation soil-DDT with different pH shows the importance of working in the acid medium.

References

1. Sharma BK (2001) Soil noise pollution, 2nd edn. Krishna Prakashan, Meerut
2. Mirsal IA (2004) Soil pollution: origin, monitoring & remediation. Springer, German
3. Misra DSG (2009) Soil pollution. APH Publishing Corporation, Delhi
4. Simeonov L, Sargsyan V (2008) Soil chemical pollution, risk assessment, remediation and security. In: Proceedings of the nato advanced research workshop on soil chemical pollution, risk assessment, remediation and security, Sofia, Bulgaria, 23–26 May 2007. Springer, Berlin
5. Houlding S (1994) Subsurface soil contamination assessment. In: Houlding SW (ed), 3d geoscience modeling. Springer, Berlin, pp 203–222. https://doi.org/10.1007/978-3-642-79012-6_12
6. FAO (2007) Assessing soil contamination: a reference manual. Daya Publishing House, Delhi

7. Pingali PL, Roger PA (1995) Impact of pesticides on farmer health and the rice environment. Kluwer Academic Publishers, Dordrecht
8. Garcia M (2004) Effects of pesticides on soil fauna: development of ecotoxicological test methods for tropical regions. Cuvillier
9. Sudharshan S, Naidu R, Mallavarapu M, Bolan N (2012) DDT remediation in contaminated soils: a review of recent studies. *Biodegradation* 23(6):851–863. <https://doi.org/10.1007/s10532-012-9575-4>
10. Zhang Y, Wong JWC, Zhao Z, Selvam A (2011) Microemulsion-enhanced remediation of soils contaminated with organochlorine pesticides. *Environ Technol* 32(16):1915–1922. <https://doi.org/10.1080/09593330.2011.568009>
11. Rios LE (2010) Removal of DDT from soil using combinations of surfactants. Thesis, University of Waterloo, Waterloo, Ontario, Canada
12. Wang X-P, Sheng J-J, Gong P, Xue Y-G, Yao T-D, Jones KC (2012) Persistent organic pollutants in the tibetan surface soil: spatial distribution, air-soil exchange and implications for global cycling. *Environ Pollut* 170:145–151. <https://doi.org/10.1016/j.envpol.2012.06.012>
13. Tremolada P, Comolli R, Parolini M, Moia F, Binelli A (2011) One-year cycle of DDT concentrations in high-altitude soils. *Water Air Soil Pollut* 217(1–4):407–419. <https://doi.org/10.1007/s11270-010-0596-5>
14. Dai R-L, Zhang G-Y, Gu X-Z, Wang M (2008) Sorption of 1,1,1-trichloro-2,2-bis(p-chlorophenyl) ethane (DDT) by clays and organoclays. *Environ Geochem Health* 30(5):479–488. <https://doi.org/10.1007/s10653-007-9130-0>
15. Calow P (2004) Euro chlor risk assessment for the marine environment osparcom region: north sea. Kluwer academic, dordrecht
16. Rodriguez-Morales AJ, Benítez JA, Arria M (2007) Malaria mortality in Venezuela: focus on deaths due to plasmodium vivax in children. *J Trop Pediatr* 54(2):94–101
17. McGinn AP (2002) Malaria, mosquitoes, and DDT: the toxic war against a global disease. WORLD•WATCH. Worldwatch Institute, Washington
18. Gautam SK, Suresh S (2007) Studies on dechlorination of DDT (1,1,1-trichloro-2,2-bis(4-chlorophenyl)ethane) using magnesium/palladium bimetallic system. *J Hazard Mater* 139(1):146–153. <https://doi.org/10.1016/j.jhazmat.2006.06.017>
19. Pushpavanam S (2002) Introduction to Chemical Engineering. PHI Learning, Delhi
20. Hajjar MJ (2012) The persisted organic pesticides pollutant (POPs) in the Middle East Arab Countries. *Int J Agron Plant Prod* 3(1):11–18
21. Ewing AE (2003) Water quality and public health monitoring of surface waters in the Kura-Araks river basin of Armenia, Azerbaijan and Georgia. Water Resources Program, University of New Mexico, Albuquerque
22. Howard PH (1991) Handbook of environmental fate and exposure data: for organic chemicals, volume III pesticides. Taylor & Francis, London
23. Zhongming G, Xuejun W, Bengang L, Jun C, Fuliu X, Yanhong C, Wenju Z, Weiran S, Baoping Q, Ren S, Zuo T (2003) The residues distribution of DDT and its metabolites in soils from Tianjin region, China. *Acta Sci Circumst* 23(4):447–451
24. Gong Z, Wang X, Li B, Cao J, Xu F, Cui Y, Zhang W, Shen W, Qin B, Sun Y, Tao S (2003) The residues distribution of DDT and its metabolites in soils from Tianjin region, China. *Acta Sci Circumst* 23(4):447–451
25. Taha OME, Taha MR (2015) Soil-water characteristic curves and hydraulic conductivity of nanomaterial-soil-bentonite mixtures. *Arab J Geosci* 9(1):12. <https://doi.org/10.1007/s12517-015-2038-6>
26. Taha M, Taha O (2012) Influence of nano-material on the expansive and shrinkage soil behavior. *J Nanopart Res* 14(10):1–13. <https://doi.org/10.1007/s11051-012-1190-0>
27. Varanasi P, Fullana A, Sidhu S (2007) Remediation of PCB contaminated soils using iron nano-particles. *Chemosphere* 66(6):1031–1038. <https://doi.org/10.1016/j.chemosphere.2006.07.036>
28. Reyes CR, Appasamy D, Roberts C (2011) An integrated remediation system using synthetic and natural zeolites for treatment of wastewater and contaminated sediments. *Dynamics* 78:125–134
29. Shanableh A, Kharabsheh A (1996) Stabilization of Cd, Ni and Pb in soil using natural zeolite. *J Hazard Mater* 45(2–3):207–217. [https://doi.org/10.1016/0304-3894\(95\)00093-3](https://doi.org/10.1016/0304-3894(95)00093-3)
30. Gholikandi GB, Baneshi MM, Dehghanifard E, Salehi S, Yari AR (2010) Natural zeolites application as sustainable adsorbent for heavy metals removal from drinking water. *Iran J Toxicol* 3(3):302–310
31. Tahir H, Uddin F (2005) Estimation of Pb from metal and electroplating industrial waste by zeolite-3a. *J Appl Sci Environ Manag* 9(2):49–55. <http://dx.doi.org/10.4314/jasem.v9i2.17290>
32. Shi W-Y, Shao H-B, Li H, Shao M-A, Du S (2009) Progress in the remediation of hazardous heavy metal-polluted soils by natural zeolite. *J Hazard Mater* 170(1):1–6. <https://doi.org/10.1016/j.jhazmat.2009.04.097>
33. Burlakovs J, Klavins M, Karklina A (2012) Remediation of soil contamination with heavy metals by using zeolite and humic acid additives. *Latv J Chem*. <https://doi.org/10.2478/v10161-012-0019-6>
34. Sayed SA (1996) Exchange of Zn²⁺, V²⁺, Cd²⁺, and Hg₂⁺ using zeolite a and dinonylnaphthalenesulfonate. *Zeolites* 17(3):261–264. [https://doi.org/10.1016/0144-2449\(96\)00040-1](https://doi.org/10.1016/0144-2449(96)00040-1)
35. Samarghandi MR, Al-Musawi TJ, Mohseni-Bandpi A, Zarrabi M (2015) Adsorption of cephalixin from aqueous solution using natural zeolite and zeolite coated with manganese oxide nanoparticles. *J Mol Liq* 211(Supplement C):431–441. <https://doi.org/10.1016/j.molliq.2015.06.067>
36. Mohseni-Bandpi A, Al-Musawi TJ, Ghahramani E, Zarrabi M, Mohebi S, Vahed SA (2016) Improvement of zeolite adsorption capacity for cephalixin by coating with magnetic Fe₃O₄ nanoparticles. *J Mol Liq* 218(Supplement C):615–624. <https://doi.org/10.1016/j.molliq.2016.02.092>
37. Qiu H, Lv L, Pan B-C, Zhang Q-J, Zhang W-M, Zhang Q-X (2009) Critical review in adsorption kinetic models. *J Zhejiang Univ Sci A* 10(5):716–724. <https://doi.org/10.1631/jzus.A0820524>
38. Tan IAW, Ahmad AL, Hameed BH (2009) Adsorption isotherms, kinetics, thermodynamics and desorption studies of 2,4,6-trichlorophenol on oil palm empty fruit bunch-based activated carbon. *J Hazard Mater* 164(2–3):473–482. <https://doi.org/10.1016/j.jhazmat.2008.08.025>
39. Ho YS, McKay G (1999) Pseudo-second order model for sorption processes. *Process Biochem* 34(5):451–465. [https://doi.org/10.1016/S0032-9592\(98\)00112-5](https://doi.org/10.1016/S0032-9592(98)00112-5)
40. Kalthori EM, Al-Musawi TJ, Ghahramani E, Kazemian H, Zarrabi M (2017) Enhancement of the adsorption capacity of the light-weight expanded clay aggregate surface for the metronidazole antibiotic by coating with mgo nanoparticles: studies on the kinetic, isotherm, and effects of environmental parameters. *Chemosphere* 175(Supplement C):8–20. <https://doi.org/10.1016/j.chemosphere.2017.02.043>
41. Shahmohammadi-Kalalagh S, Babazadeh H, Nazemi AH, Man-shouri M (2011) Isotherm and kinetic studies on adsorption of Pb, Zn and Cu by kaolinite. *Casp J Environ Sci* 9(2):243–255

42. Ho YS, McKay G (1998) Sorption of dye from aqueous solution by peat. *Chem Eng J* 70(2):115–124. [https://doi.org/10.1016/S0923-0467\(98\)00076-1](https://doi.org/10.1016/S0923-0467(98)00076-1)
43. Tütem E, Apak R, Ünal ÇF (1998) Adsorptive removal of chlorophenols from water by bituminous shale. *Water Res* 32(8):2315–2324. [https://doi.org/10.1016/S0043-1354\(97\)00476-4](https://doi.org/10.1016/S0043-1354(97)00476-4)
44. Samadi MT, Rahman AR, Zarrabi M, Shahabi E, Sameei F (2009) Adsorption of chromium (VI) from aqueous solution by sugar beet bagasse-based activated charcoal. *Environ Technol* 30(10):1023–1029. <https://doi.org/10.1080/09593330903045107>
45. Wu F-C, Tseng R-L, Juang R-S (2001) Kinetic modeling of liquid-phase adsorption of reactive dyes and metal ions on chitosan. *Water Res* 35(3):613–618. [https://doi.org/10.1016/S0043-1354\(00\)00307-9](https://doi.org/10.1016/S0043-1354(00)00307-9)
46. Yang X, Al-Duri B (2005) Kinetic modeling of liquid-phase adsorption of reactive dyes on activated carbon. *J Colloid Interface Sci* 287(1):25–34. <https://doi.org/10.1016/j.jcis.2005.01.093>
47. Weber WJ, Morris JC (1962) Advances in water pollution research: removal of biologically resistant pollutants from waste waters by adsorption. In: Proceedings of international conference on water pollution symposium. Pergamon Press, Oxford, pp 231–266
48. Alkan M, Demirbaş Ö, Doğan M (2007) Adsorption kinetics and thermodynamics of an anionic dye onto sepiolite. *Microporous Mesoporous Mater* 101(3):388–396. <https://doi.org/10.1016/j.micromeso.2006.12.007>
49. Zeldowitsch J (1934) Über Den Mechanismus Der Katalytischen Oxydation Von Co an MnO_2 . *Acta Physicochem URSS*
50. Yakout SM, Elsharif E (2010) Batch kinetics, isotherm and thermodynamic studies of adsorption of strontium from aqueous solutions onto low cost rice-straw based carbons. *Carbon Sci Technol* 3(1):144–153
51. Yousef RI, El-Eswed B, Al-Muhtaseb AAH (2011) Adsorption characteristics of natural zeolites as solid adsorbents for phenol removal from aqueous solutions: kinetics, mechanism, and thermodynamics studies. *Chem Eng J* 171(3):1143–1149. <https://doi.org/10.1016/j.cej.2011.05.012>
52. Bhattacharyya R, Ray SK (2013) Kinetic and equilibrium modeling for adsorption of textile dyes in aqueous solutions by carboxymethyl cellulose/poly(acrylamide-Co-hydroxyethyl methacrylate) semi-interpenetrating network hydrogel. *Polym Eng Sci* 53(11):2439–2453. <https://doi.org/10.1002/pen.23501>
53. Temkin MJ, Pyzhev V (1940) Kinetics of ammonia synthesis on promoted iron catalysts. *Acta Physicochim* 12:217–222
54. Mall ID, Srivastava VC, Agarwal NK (2006) Removal of orange-G and methyl violet dyes by adsorption onto bagasse fly ash—kinetic study and equilibrium isotherm analyses. *Dyes Pigment* 69(3):210–223. <https://doi.org/10.1016/j.dyepig.2005.03.013>
55. Bhatnagar A (2007) Removal of bromophenols from water using industrial wastes as low cost adsorbents. *J Hazard Mater* 139(1):93–102. <https://doi.org/10.1016/j.jhazmat.2006.06.139>
56. Sepehr MN, Yetilmezsoy K, Marofi S, Zarrabi M, Ghaffari HR, Fingas M, Foroughi M (2014) Synthesis of nanosheet layered double hydroxides at lower pH: optimization of hardness and sulfate removal from drinking water samples. *J Taiwan Inst Chem Eng* 45(5):2786–2800. <https://doi.org/10.1016/j.jtice.2014.07.013>
57. Húmpola PD, Odetti HS, Ferrúta AE, Vicente JL (2013) Thermodynamic analysis of adsorption models of phenol in liquid phase on different activated carbons. *J Chil Chem Soc* 58(1):1541–1544. <https://doi.org/10.4067/S0717-97072013000100009>
58. Pan B, Xing B (2008) Adsorption mechanisms of organic chemicals on carbon nanotubes. *Environ Sci Technol* 42(24):9005–9013. <https://doi.org/10.1021/es801777n>
59. Soori MM, Ghahramani E, Kazemian H, Al-Musawi TJ, Zarrabi M (2016) Intercalation of tetracycline in nano sheet layered double hydroxide: an insight into UV/Vis spectra analysis. *J Taiwan Inst Chem Eng* 63(Supplement C):271–285. <https://doi.org/10.1016/j.jtice.2016.03.015>
60. Poursaberi T, Konozb E, Sarrafi AHM, Hassanisadi M, Hajifathli F (2012) Application of nanoscale zero-valent iron in the remediation of DDT from contaminated water. *Chem Sci Trans* 1(3):658–668. <https://doi.org/10.7598/cst2012.246>